Electronic Spectrum of Tin Oxide: MRDCI Study

Dipankar Giri,[†] Robert J. Buenker,[‡] and Kalyan Kumar Das*[,†]

Department of Chemistry, Physical Chemistry Section, Jadavpur University, Kolkata 700 032, India, and FB-9, Theoretische Chemie, Bergische Universität Wuppertal, Gaussstrasse 20, D-42097 Wuppertal, Germany

Received: April 5, 2002; In Final Form: June 6, 2002

Multireference singles and doubles configuration interaction (MRDCI) calculations have been carried out to investigate the electronic structure and spectroscopic properties of the low-lying electronic states of tin oxide. A sufficiently large basis set with additional d and f polarization functions is employed. Potential energy curves of both spin-excluded and spin-included states, which correlate with the lowest dissociation limit $Sn(^3P_g)+O(^3P_g)$, are reported. The computed spectroscopic properties of the electronic states below 40 000 cm^{-1}, such as $X^1\Sigma^+$, a $^3\Sigma^+$, $b^3\Pi$, $A^1\Pi$, $E^1\Sigma^+$, and their spin−orbit components, are compared with the observed results. The MRDCI estimated dissociation energy of the ground state of SnO is 5.03 eV taking the d-correlation into account. Effects of the d-electron correlation on the spectroscopic constants of the ground and a few low-lying Λ−S states have been explored. Transition probabilities of a few transitions are estimated. The $A^1\Pi-X$ and $E^1\Sigma^+-X$ transitions are predicted to be quite strong. The spin-forbidden transitions such as $b^3\Pi_1-X$ and $b\ ^3\Pi_{0^+}-X$ are compared with the Cameron band of the isovalent CO molecule. The calculated dipole moments of SnO as a function of the bond length in three low-lying states, namely $X^1\Sigma^+$, $A^1\Pi$, and $E^1\Sigma^+$, have been reported.

I. Introduction

Over the past several decades, a large number of experimental studies[1−17] has been carried out on the diatomic oxides, halides, nitrides, and hydrides of group IVA, as these compounds are good candidates for a chemical laser.[1] In this regard, SnO is significant because of 50% photon yields from the Sn + N_2O reaction.[2] Spectroscopic properties of several excited states and the thermochemical dissociation energy of SnO have been reported in early thirties.[3] Jevons[4] has studied UV band systems, namely, A−X, B−X, and C−X of GeO, SnO, and PbO. Lagerqvist et al.[5] have made rotational analyses of the A−X system of SnO to establish it as due to the $^1\Pi-^1\Sigma^+$ transition which is similar to the spectra of isovalent molecules, such as CO, CS, SiO, SiS, etc. The band-origin has been observed at ν_{00} = 29 503.2 cm^{-1}. Sometimes, this band has been denoted as D−X. The ultraviolet E−X system has been investigated long ago[6,7] with a band-origin at ν_{00} = 36 138 cm^{-1}. The E−X system corresponds to the $^1\Sigma^+-^1\Sigma^+$ transition. Later on, Eisler and Barrow[8] have extended the vibrational analysis of the E−X system from the absorption exposure of tin oxide. The absorption spectra of the gaseous SiO, GeO, and SnO in the Schumann region have allowed the spectroscopic constants and dissociation products of many low-lying excited states to be determined.[9] In SnO, Deutsch and Barrow[10] have observed $^3\Pi_1 \leftarrow X^1\Sigma^+_{0^+}$ and $^3\Pi_{0^+} \leftarrow X^1\Sigma^+_{0^+}$ transitions which are analogous to the strongest spin-forbidden Cameron band $b^3\Pi-X^1\Sigma^+$ observed in CO. Nair et al.[11] have calculated potential energy curves and dissociation energies of oxides and sulfides of group IVA elements from the experimental energy levels using semiclassical methods. The $D^1\Pi-X^1\Sigma^+$ absorption systems for SnS and SnO are reported[12] in the 14 000−50 000 cm^{-1} region in inert gas matrices at low temperature. The excitation into the D state of both oxide and sulfide has yielded a strong red fluorescence which has been attributed to the $a^3\Pi-X$ transition. Meyer et al.[13] have measured the lifetimes of the Cameron bands of isovalent GeO, GeS, SnO, and SnS in inert gas matrices at low temperature. The lifetimes of these bands fall between 100 μs and 3 ms. The gas-phase lifetimes of the excited $^3\Pi$ states are also estimated for these molecules.

The emission spectra from flames containing halides or metallic tin has been investigated by Joshi and Yamdagni[14] in the visible region. A large number of bands has been attributed to SnO, and the complete spectrum above 350 nm has been divided into four systems, A−X, B−X, C−X, and D−X. Using the technique of photographic photometry, Dube and Rai[15] have measured the relative band intensities of the vibrational bands in the $D^1\Pi-X^1\Sigma^+$ system of SnO. Einstein coefficients and oscillator strengths for this system have been also measured from the observed data. Capelle and Linton[16] have studied chemiluminescence spectra and photon yields for several Sn-oxidizer reactions. A new band of the $a^3\Sigma^+_1-X^1\Sigma^+$ system of SnO has been reported with T_e = 20 622.6 ± 2.5 cm^{-1} and ω_e = 554.0 ± 1.7 cm^{-1} for the $a^3\Sigma^+_1$ state. These authors have measured the intensity of photoluminescence signal from pulse N_2 laser excitation of SnO at different time for several total system pressures. The $a^3\Sigma^+_1$, $b(0^+)$, and b′(1) states, which correlate with the low-lying triplets, are expected to be relatively long-lived. The infrared spectra of many isovalent matrix-isolated germanium, tin, and lead monochalcogenides have been carried out by Marino et al.[17]

Although there are many experimental studies for the low-lying electronic states of SnO, theoretical investigations are less in number. Balasubramanian and Pitzer[18] are the first to have undertaken relativistic quantum mechanical calculations at the configuration interaction (CI) level with spin−orbit coupling for seven low-lying states of SnO. Some of the observed states

* Author for correspondence. E-mail: kalyankd@hotmail.com, das_kalyank@yahoo.com, and kalyankd@vsnl.net.
† Department of Chemistry.
‡ Theoretische Chemie.

10.1021/jp020912i CCC: $22.00
Published on Web 08/16/2002

have been compared with the calculated results. In a subsequent study, Balasubramanian[19] has carried out SCF/RCI calculations on the low-lying electronic states of SnO^+ as well as heavier ions such as PbO^+, PbS^+, and $PbSe^+$. Dyke et al.[20] have recorded the gas-phase high-temperature photoelectron spectrum of the SnO molecule in the ground state. This study has provided ionization energies of the molecule. Relativistic CI calculations of heavy molecules and clusters have been reviewed by Balasubramanian.[21−23] Recently, Kellö et al.[24] have performed coupled cluster calculations with single and double excitations and perturbative corrections for the contribution of triple excitations [CCSD(T)] to evaluate electron correlation contributions to the dipole moments of SnO, PbO, SnS, and PbS. The computed dipole moment of SnO has been found to be −1.59 ea_0 at the equilibrium bond length.[24] Similar but less accurate calculations have found −1.44 ea_0 as the dipole moment of SnO.[25] The electronic structures of tin monochalcogenide (SnX, X = O, S, Se, and Te) crystals have been calculated by Lefebvre et al.[26] by using density functional pseudopotential and tight binding theories. Ab initio based MRDCI calculations on the low-lying electronic states of isovalent molecules such as SiS, GeS, GeSe, and GeTe have been performed recently[27−30] using relativistic effective core potentials.[31−34] These calculations have described the spectroscopic properties and potential energy curves of a large number of electronic states with and without spin−orbit coupling.

The structural and spectroscopic properties of low-lying electronic states of SnO have been studied in this work by using MRDCI calculations with relativistic effects including the spin−orbit interaction. Transition moments of some observed transitions are computed. Of these, the A−X, E−X, and b−X transitions are given special attention. Radiative lifetimes of a few low-lying states of SnO are also estimated in this study.

II. Methodological Details

Tin, being a heavy atom, requires the use of effective potentials for the CI calculations of its molecules. The semicore relativistic effective core potential (RECP) of Sn has been taken from LaJohn et al.,[35] in which $4d^{10}5s^25p^2$ electrons of the atom are kept in the valence space, while the remaining inner electrons are described by means of effective potentials. Thus the number of active electrons for Sn is 14. For the oxygen atom, we have used the RECP of Pacios and Christiansen,[36] which include $2s^22p^4$ electrons in the valence space. The total number of active electrons to be treated in the CI calculations of SnO is 20. The primitive Gaussian basis for Sn, compatible with the above-mentioned semicore RECP, is 3s3p4d without any contraction. But the set of basis functions of the Sn atom is augmented with d and f polarization functions having optimized exponents of 0.08 and 0.20 a_0^{-2}, respectively.[37] Additionally, one set of diffuse s(ζ=0.015 a_0^{-2}) and p(ζ=0.012 a_0^{-2}) functions are included in the basis set. This makes the final AO basis functions of Sn to be 4s4p5d1f in the uncontracted form. For the oxygen atom, the 4s4p basis set of Pacios and Christiansen[36] is augmented with d functions of optimized[38] exponent of 1.33 a_0^{-2}. Therefore, the final basis set used here for oxygen is 4s4p1d without any contraction.

Using the above-mentioned basis functions of Sn and O, we have carried out a set of self-consistent-field (SCF) calculations at each internuclear distance to generate reasonably good optimized symmetry adapted molecular orbitals to be used for CI calculations of SnO. The molecule has been kept along the +z axis with Sn at the origin. The computations are performed in the C_{2v} symmetry in order to take the advantage of the simplicity of the Abelian group direct product relationship.

Several tests have been made before choosing the proper state for the SCF-MO calculations. It is known[18,39] that the $\sigma^2\pi^4\ ^1\Sigma^+$ state, which happens to be the ground state of SnO, may not be suitable for the excited-state calculations, because the π^* MO is not occupied. To describe the excited states in a better way, one needs to optimize the π^* orbital in the SCF calculations. The SCF calculations of three other states, namely $\sigma\pi^4\pi^*\ ^3\Pi$, $\sigma^2\pi^3\pi^*\ ^3\Sigma^-$, and $\pi^4\pi^{*2}\ ^3\Sigma^-$ (excited) have been tested. Both $\sigma\pi^4\pi^*\ ^3\Pi$ and $\sigma^2\pi^3\pi^*\ ^3\Sigma^-$ states have the disadvantage of having inequivalent π_x and π_y components, but the doubly excited state of the $^3\Sigma^-$ symmetry does not pose such a problem. In the present study, we have used SCF MOs of the $\pi^4\pi^{*2}\ ^3\Sigma^-$ state for the entire CI calculations of SnO. We would like to mention that eigenvalues and eigenfunctions in B_1 and B_2 irreducible representations retain their perfect symmetries throughout the calculations. There are no symmetry breaking solutions in Π states of the molecule. The $4d^{10}$ electrons of Sn are found to be localized and do not participate in the formation of low-lying electronic states of the molecule. Hence the corresponding SCF MOs are kept frozen in the CI step, which reduces the number of active electrons to 10 for the CI calculations. However, to determine the effect of the d-correlation, CI calculations for a few bound states are repeated in the Franck−Condon region keeping d^{10} electrons of Sn in the active space.

We have employed the MRDCI method with perturbative correction and energy extrapolation techniques of Buenker and co-workers[40−46] throughout the calculations. The Table-CI algorithm[46] is used to handle the open-shell configurations which appear because of the excitation process. A set of reference configurations is chosen for low-lying excited states of a given spin and spatial symmetry. For singlet and triplet spin multiplicities, eight roots are calculated, while the number of lowest roots computed for quintets is four. All possible single and double excitations are carried out from these reference configurations. These excitations generate a large number of configurations with a maximum number of the order of 9 million. But the choice of a configuration-selection threshold T = 3.0 μE_h reduces the selected configurations to a number below 50 000. At this threshold value, the sums of the square of coefficients of the reference configurations for the lowest few roots remain above 0.90. The energy extrapolation method[40−42] allows us to estimate energies at T = 0. The effect of some higher excitations from the reference configurations has been taken care by the multireference analogue of the Davidson correction.[47,48] It may be mentioned here that some higher order excitations are still missing. However, the correction does not make much difference in the excitation energies. This will provide an estimate of the full-CI energies in the same atomic orbital basis. The calculations have been carried out from 3.0 to 15 a_0 with an increment of 0.1 a_0 in the short-range up to r = 7.0 a_0. In the longer bond length region, the increment has been set to 1.0 a_0, while in the Franck−Condon region a smaller increment of 0.05 a_0 has been used.

The spin−orbit CI calculations have been carried out by allowing all components of low-lying Λ−S states to interact. The spin−orbit operators, which are compatible with RECPs of Sn and O, are taken from LaJohn et al.[35] and Pacios and Christiansen,[36] respectively. The spin-independent MRDCI wave functions are multiplied with appropriate spin functions, which transform as C_{2v} irreducible representation. The diagonals of the spin-included Hamiltonian matrix consist of full CI energies of the Λ−S CI calculations, while the off-diagonals are calculated by the RECP-based spin−orbit operators and Λ−S

TABLE 1: Dissociation Relationship between the Molecular States and Atomic States of SnO

molecular state	atomic state Sn + O	relative energy/cm^{-1} exptl[a]	calcd
$^1\Sigma^+(2)$, $^1\Sigma^-$, $^1\Pi(2)$, $^1\Delta$	$^3P_g+^3P_g$	0	0
$^3\Sigma^+(2)$, $^3\Sigma^-$, $^3\Pi(2)$, $^3\Delta$			
$^5\Sigma^+(2)$, $^5\Sigma^-$, $^5\Pi(2)$, $^5\Delta$			
$^3\Sigma^+$, $^3\Sigma^-(2)$, $^3\Pi(3)$, $^3\Delta(2)$, $^3\Phi$	$^1D_g+^3P_g$	5764	5860

[a] Reference 52.

CI wave functions. Three representations, namely A_1, A_2, and B_1 of the C_{2v}^2 group consist of all Ω-components of the low-lying electronic states of the molecule. The sizes of the secular equations of A_1, A_2, and B_1 blocks are 25 × 25, 25 × 25, and 21 × 21, respectively for some selected number of roots of Λ−S symmetries of the molecule. Diagonalization of these spin included blocks gives the energies and wave functions of spin−orbit states. There are certain advantages in such a two step variational method for the inclusion of the spin−orbit interaction. The computational labor is much lower to achieve the desired level of accuracy. However, the main disadvantage of this simpler two-step method is that the spin−orbit term is not treated at the same level as the nonrelativistic terms. It is assumed that the scalar one-particle functions are not significantly affected by the spin−orbit term. On the other hand, the more flexible one-step or direct spin−orbit CI treatment, in which the electrostatic and spin−orbit interactions are treated on an equal footing, is computationally demanding and beyond the scope of the present calculations. The calculations of transition moments in the two-step method can be carried out easily. Moreover, the spin−orbit CI wave functions can be analyzed in terms of Λ−S eigenfunctions.

Spectroscopic properties of both spin-independent and spin-included low-lying states of SnO are obtained by fitting the corresponding potential energy curves into polynomials. The one-dimensional nuclear Schrödinger equations are solved numerically by using these polynomials to calculate vibrational energies and wave functions. These are used in the computation of transition dipole moments for the pair of vibrational functions in a particular transition. Subsequently, Einstein spontaneous emission coefficients and hence transition probabilities are calculated. Radiative lifetimes of excited states at different vibrational levels are estimated from these data.

III. Potential Curves and Spectroscopic Constants of Λ−S States

Eighteen Λ−S states of SnO correlate with the ground states (^3P_g) of both Sn and O atoms. The excited ^1D_g state of Sn interacts with the ground state of the oxygen atom to generate nine Λ−S states of triplet spin multiplicity. In Table 1, we have provided the low-lying Λ−S states correlating with the lowest two dissociation limits. The observed energy splitting $\Delta E(^3P_g-^1D_g)$ for the Sn atom agrees well with the value computed from the MRDCI calculations of the SnO molecule at a very large internuclear distance. Potential energy curves of all eighteen states which do not include the spin−orbit coupling and dissociate into the lowest asymptote $Sn(^3P_g)+O(^3P_g)$ are shown in Figure 1. There are nine Λ−S states which are bound within 35 000 cm^{-1}. Spectroscopic constants of these states of SnO are shown in Table 2. At equilibrium, the ground state ($X^1\Sigma^+$) of SnO is found to be dominated by the closed shell $\sigma^2\pi^4$ (c^2 = 0.85) configuration by using the ground-state MOs as the one-particle basis for CI. The σ MO is found to be strongly bonding combination of p_z atomic orbitals of both Sn and O, while the

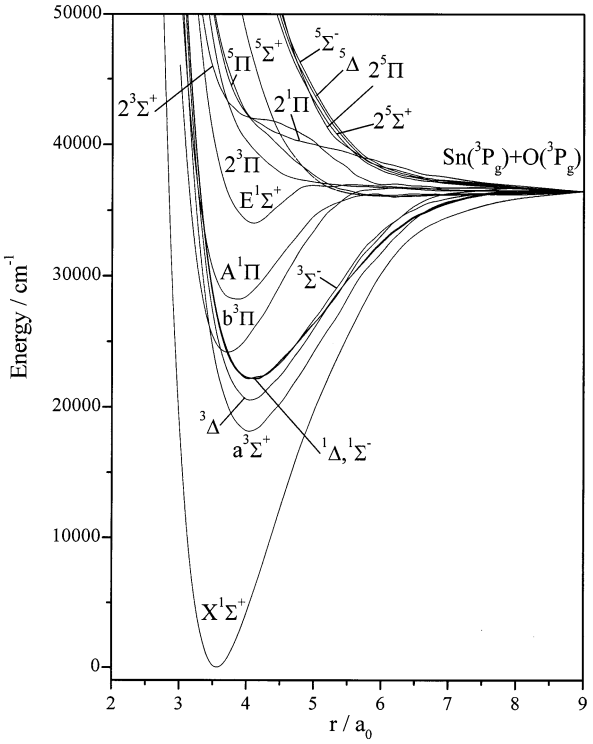

Figure 1. Computed potential energy curves of 18 Λ−S states of SnO.

TABLE 2: Spectroscopic Constants of Low-Lying Λ−S States of SnO

state	T_e/cm^{-1}	r_e/Å	ω_e/cm^{-1}
$X^1\Sigma^+$	0	1.883	758
		(1.833)[a]	(814.6)[a]
		[1.94][b]	[800][b]
$a^3\Sigma^+$	18180	2.136	504
	[18606][b]	[2.13][b]	[542][b]
$^3\Delta$	20514	2.147	489
	[20561][b]	[2.16][b]	[493][b]
$^3\Sigma^-$	22070	2.155	440
	[22750][b]	[2.15][b]	[530][b]
$^1\Delta$	22081	2.164	445
$^1\Sigma^-$	22123	2.159	446
	[22890][b]	[2.14][b]	[540][b]
$b^3\Pi$	24135	1.970	566
	[24100][b]	[2.06][b]	[770][b]
$A^1\Pi$	28174	2.030	502
	(29624)[c]	(1.948)[c]	(580)[c,e]
	(29505)[d]	(1.95)[e]	
	[26700][b]	[2.06][b]	[710][b]
$E^1\Sigma^+$	34060	2.163	490
	(36138)[a]		(508)[a]
$3^1\Pi$	53586	2.066	557

[a] Reference 49. [b] Reference 18. [c] Reference 5. [d] Reference 16. [e] Reference 15.

π MO is strongly localized on the $p_{x/y}$ atomic orbitals of the oxygen atom. However, $p_{x/y}$(Sn) atomic orbitals contribute to a small extent in the bonding combination with $p_{x/y}$(O). On the other hand, the π^* MO is weakly antibonding with its charge distribution more localized on the Sn atom. It is true that the form of multireference function sometimes depends on the choice of one particle basis function. This has been reflected in the CI calculations of the ground state of SnO. Using the MOs of the $\pi^4\pi^{*2}$ $^3\Sigma^-$ state, the ground state of SnO shows a two-configuration character. Except $E^1\Sigma^+$, other low-lying states of SnO are mostly found to be dominated by a single configuration and do not depend on the choice of the one-particle basis functions. The MRDCI estimated r_e of the ground state of SnO

is 0.05 Å longer than the experimental[49] value of 1.833 Å. However, our value shows better agreement than the value of 1.94 Å obtained by Balasubramanian and Pitzer.[18] The vibrational frequency of the ground state at r_e is computed to be 758 cm^{-1} as compared with the observed[49] value of 814.6 cm^{-1}. A set of CI calculations which include d^{10} electrons of Sn in the excitation process at higher threshold $T = 5.0$ μhartrees has been performed. The Franck−Condon region and dissociation limits for the ground and a few low-lying Λ−S states are studied with 20 electrons in CI. The equilibrium bond length of the ground state is improved by 0.02 Å, while ω_e is increased by 53 cm^{-1}. Except for Π states, transition energies and vibrational frequencies are generally increased by 650−1500 cm^{-1} and 20−70 cm^{-1}, respectively, while the equilibrium bond lengths are reduced by 0.02−0.04 Å.

The first excited state of SnO is of a $^3\Sigma^+$ symmetry. The observed a−X system[16] for SnO has yielded spectroscopic constants of a $^3\Sigma^+(1)$ as $T_e = 20\,622.6 \pm 2.5$ cm^{-1} and $\omega_e = 554.0 \pm 1.7$ cm^{-1}. The computed transition energy of the $a^3\Sigma^+$ state without any spin−orbit coupling is found to be 18 180 cm^{-1}. The experimental r_e of the $a^3\Sigma^+$ state of SnO is not available for comparison. However, we expect that the MRDCI estimated r_e would be larger by 0.02−0.05 Å. The $a^3\Sigma^+$ state of SnO is analogous to the $a'^3\Sigma^+$ state of the isovalent CO molecule. The MRDCI wave functions show that the $a^3\Sigma^+$ state of SnO is characterized mainly by singly excited configuration ($\pi \rightarrow \pi^*$). The state is reasonably strongly bound with a binding energy of 2.35 eV obtained from the MRDCI treatment. The $\pi^3\pi^*$ configuration is expected to generate other five Λ−S states which are identified as $^3\Delta$, $^3\Sigma^-$, $^1\Delta$, $^1\Sigma^-$, and $^1\Sigma^+$. Figure 1 and Table 2 show that all five other states converge to the lowest asymptote of the SnO molecule. The first four of these, namely, $^{1,3}\Delta$ and $^{1,3}\Sigma^-$, are found to be almost pure single-configuration states, while the second $^1\Sigma^+$ state, designated as $E^1\Sigma^+$, is described by several configurations. It is found that the $\sigma\sigma'\pi^3\pi^*$ excited configuration in which σ' is an admixture of bonding s and antibonding p orbitals of Sn and O contributes to a small extent in all the above-mentioned five states. The $^{1,3}\Sigma^-$ and $^1\Delta$ states are nearly degenerate around 22 000 cm^{-1}, while the $^3\Delta$ state is found to lie 2500 cm^{-1} below these states (see Figure 1). None of these four states is experimentally observed. However, $^3\Sigma^-_{0^+,1}-X^1\Sigma^+_{0^+}$ transitions are expected to take place around 22 000 cm^{-1}. Other spectroscopic constants, namely, r_e and ω_e of $^{1,3}\Delta$ and $^{1,3}\Sigma^-$, are very similar in magnitude, and all these states are found to be very strongly bound.

The $b^3\Pi$ state of SnO is the next important state which is bound by about 12 000 cm^{-1}. The $^3\Pi-X^1\Sigma^+$ band, which is similar to the spin-forbidden Cameron band of CO, has been spectroscopically investigated from the rotational analysis. The transition energies of the $b^3\Pi_{0^+,1}-X^1\Sigma^+$ transitions of SnO are known experimentally. According to the MRDCI calculations, the $b^3\Pi$ state lies around 24 135 cm^{-1} with $r_e = 1.97$ Å and $\omega_e = 566$ cm^{-1}. Spectroscopic constants of the spin−orbit components of $b^3\Pi$ agree well with the calculated values. This will be discussed in the next section. The CI wave function of the $b^3\Pi$ state in the Franck−Condon region is dominated by the $\sigma\pi^4\pi^*$ configuration, but nearly 10% doubly excited configurations such as $\sigma\pi^3\pi^{*2}$ contribute to the formation of the $b^3\Pi$ state. Since the σ MO is strongly bonding with respect to the p_z atomic orbitals of Sn and O, the $\sigma \rightarrow \pi^*$ excitation makes the Sn−O bond in the $b^3\Pi$ state weaker than the ground-state bond. As seen in Table 2, the present T_e value of the $b^3\Pi$ state is in excellent agreement with the value reported by Balasubramanian and Pitzer,[18] but their r_e and ω_e values are overestimated to some extent. The same $\sigma \rightarrow \pi^*$ excitation results in the singlet counterpart of $b^3\Pi$. We designate the state as $A^1\Pi$, which is the most widely studied excited state of SnO. The $A^1\Pi-X^1\Sigma^+$ band is well-known not only for SnO, but also for other isovalent molecules, such as SiO, GeO, SiS, etc. In earlier studies, this band was designated as $D^1\Pi-X^1\Sigma^+$. The MRDCI estimated transition energy of the $A^1\Pi$ state is underestimated by about 1325 cm^{-1} as compared to $\nu_{00} = 29\,503.2$ cm^{-1} observed recently. The calculated r_e is shorter than the experimentally derived value by 0.08 Å, while ω_e is larger by 72 cm^{-1}. The d-correlation is expected to improve r_e by 0.02−0.04 Å. The composition of the $A^1\Pi$ state is found to be very similar to that of the $b^3\Pi$ state. The spectroscopic constants of the $A^1\Pi$ state computed here are in somewhat better agreement than other theoretical results available in the literature.[18] The A−X transition is expected to be quite strong. We shall discuss the quantitative aspect of this transition probability later on.

The next electronic state, which would undergo a strong transition, is the excited $E^1\Sigma^+$ state. The observed E−X band system has provided $T_{00} = 36\,138$ cm^{-1} as compared with the computed value of 34 060 cm^{-1}. However, the calculated ω_e value of 490 cm^{-1} agrees well with the experimentally derived value of 508 cm^{-1}. The $E^1\Sigma^+$ state dissociates into the lowest asymptote $Sn(^3P_g)+O(^3P_g)$. The potential minimum of the state is expected to be around 2.163 Å. However, the state is very weakly bound with a binding energy of only 0.3 eV, and in the Franck−Condon region, the state is represented dominantly by the $\pi^3\pi^*$ configuration. The closed shell π^4 and two other excited configurations also contribute to the $E^1\Sigma^+$ state. The multiconfiguration feature of the $E^1\Sigma^+$ state is not found to alter with other choices of the one-particle basis in CI. The 20-electron CI calculations with $T = 5.0$ μhartrees reduce r_e by 0.03 Å, while the transition energy is increased by about 1500 cm^{-1}. All six quintet states dissociating into the lowest asymptote are found to be repulsive in nature. There is a gap of at least 15 000 cm^{-1} above the $E^1\Sigma^+$ state before the next bound state is found for SnO. The $3^1\Pi$ state is bound with a potential minimum around 2.066 Å. The calculated transition energy at r_e is 53 586 cm^{-1} with $\omega_e = 557$ cm^{-1} after fitting the diabatic potential curve. Barrow and Rowlinson[9] have reported unidentified absorption bands in the range 53 250−57 670 cm^{-1} and also an absorption continuum between 51 630 and 51 920 cm^{-1}. The $3^1\Pi$ state may fit this description, and it is found to undergo a strong transition to the ground state. The potential energy curve of the $3^1\Pi$ state (not shown in Figure 1) has several avoided crossings. The state is predominantly represented by $\sigma^2\sigma_R\pi^3$ ($c^2 = 0.63$) and $\sigma^2\sigma'_R\pi^3$ ($c^2 = 0.16$) configurations, in which both σ_R and σ'_R are found to be nonbonding Rydberg type orbitals localized on Sn.

The dissociation energy of SnO obtained from the mass spectrometric study of the vaporization of tin oxides[50] has been found to be 5.49 ± 0.09 eV. The extrapolation of the E−X ($v''=0$) progression gives a dissociation limit at 45 770 cm^{-1}.[9,49] Assuming that the above limit corresponds to $^3P_1+^3P_1$, the ground-state dissociation energy of SnO has been suggested to be 5.45 eV. The estimated ground-state dissociation energy of SnO from 20-electron CI claculations has been found to be 5.03 eV which is lower than the observed value by 0.42 eV. Such a discrepancy is expected for the MRDCI method employed here. The use of the effective core potential approximation and size of the basis set are the possible sources of error.

IV. Spectroscopic Properties of Ω States

In the present calculations, we have allowed all 18 Λ−S states correlating with the lowest dissociation limit $Sn(^3P_g)+O(^3P_g)$

TABLE 3: Spectroscopic Constants of Low-Lying Ω States of SnO

state	T_e/cm^{-1}	r_e/Å	ω_e/cm^{-1}	composition at r_e (% contribution)
$X^1\Sigma^+_{0^+}$	0	1.885	755	$X^1\Sigma^+$(99)
$a^3\Sigma^+_1$	17867	2.137	492	$a^3\Sigma^+$(92), $^3\Sigma^-$(8)
	(20623)[a]		(554)[a]	
$a^3\Sigma^-_{0^+}$	17955	2.138	506	$a^3\Sigma^+$(94), $^1\Sigma^-$(5)
$^3\Delta_1$	19680	2.147	456	$^3\Delta$(99)
$^3\Delta_2$	20112	2.152	430	$^3\Delta$(71), $^1\Delta$(29)
$^3\Delta_3$	21860	2.144	457	$^3\Delta$(99)
$^3\Sigma^-_{0^+}$	22084	2.158	440	$^3\Sigma^-$(98)
$^1\Sigma^-_{0^-}$	22453	2.159	444	$^1\Sigma^-$(93), $a^3\Sigma^+$(6)
$^3\Sigma^-_1$	22490	2.155	440	$^3\Sigma^-$(92), $a^3\Sigma^+$(7)
$^1\Delta_2$	23002	2.172	431	$^1\Delta$(76), $^3\Delta$(23)
$b^3\Pi_{0^-}$	23161	1.975	561	$^3\Pi$(97), $a^3\Sigma^+$(2)
$b^3\Pi_{0^+}$	23227	1.971	569	$^3\Pi$(91), $^3\Sigma^-$(8)
	(24200)[b]	(2.008)[c]	(555)[b]	
$b^3\Pi_1$	24031	1.975	556	$^3\Pi$(75), $^3\Sigma^-$(17), $A^1\Pi$(4)
	(24760)[b]	(1.992)[c]	(560)[b]	
$b^3\Pi_2$	25233	1.963	588	$^3\Pi$(51), $^1\Delta$(40), $^3\Delta$(9)
$A^1\Pi_1$	28522	2.026	501	$A^1\Pi$(93), $^3\Pi$(7)
$E^1\Sigma^+_{0^+}$	34246	2.164	495	$E\ ^1\Sigma^+$(98), $^3\Pi$(1)

[a] Reference 16. [b] Reference 10. [c] Reference 49.

to interact through the spin−orbit coupling. 50 Ω states of 0^+, 0^-, 1, 2, 3, and 4 symmetries split into nine asymptotes within 3650 cm^{-1}. In Figure 2a−d, we have plotted computed potential energies of bound Ω components whose spectroscopic constants are given in Table 3. There are 16 Ω states within 35 000 cm^{-1} of energy. The ground-state component ($X^1\Sigma^+_{0^+}$) remains unchanged by the spin−orbit coupling. In the Franck−Condon region, there are no suitable 0^+ components which can couple with the $X^1\Sigma^+_{0^+}$ state. The $\Omega = 0^-$ and 1 components of $a^3\Sigma^+$ are separated by only 88 cm^{-1}. The computed transition energy of a $^3\Sigma^+_1$ is found to be much lower than the observed value[16] reported from the extension of the a−X system of the SnO molecule. The intensity of the a $^3\Sigma^+_1-X^1\Sigma^+_{0^+}$ transition is expected to be very small. The computed ω_e value of the a $^3\Sigma^+_1$ component is also smaller than the observed value of 554 cm^{-1}. The $a^3\Sigma^+_1$ state interacts weakly with the $^3\Sigma^-_1$ component, while a $^3\Sigma^-_{0^+}$ is coupled with the $^1\Sigma^-_{0^+}$ component having $c^2 = 0.05$. Three Ω components of $^3\Delta$ split in the energy order $^3\Delta_1 < {}^3\Delta_2 < {}^3\Delta_3$. The largest splitting has been found to be about 2200 cm^{-1}. In the Franck−Condon region, the $^3\Delta_2$ component interacts strongly with $^1\Delta_2$, while 1 and 3 components of $^3\Delta$ remain pure. The spin−orbit coupling does not greatly influence 0^+ and 1 components of $^3\Sigma^-$. The $^1\Sigma^-_{0^-}$ component lies very close to the $^3\Sigma^-_1$ component. It has been found that the spin−orbit components of a $^3\Sigma^+$ are coupled with $^1\Sigma^-_{0^-}$ and $^3\Sigma^-_1$ to a small extent. Both $^3\Sigma^-_{0^+}-X$ and $^3\Sigma^-_1-X$ transitions are, however, expected to be weak in intensities. Spectroscopic constants of all four components of $b^3\Pi$ are obtained from the diabatic curve fittings. The spin−orbit splitting of the $b^3\Pi$ state is found to be in a regular order. The maximum energy separation among these spin−orbit components is calculated to be around 2000 cm^{-1}. Around the equilibrium, there are several avoided curve-crossings for all four components of $b^3\Pi$. However, we have estimated spectroscopic parameters from the diabatic curves. Two components such as $b^3\Pi_{0+}$ and $b^3\Pi_1$ are suitable for undergoing transitions to the ground-state component. Both $b^3\Pi_1-X^1\Sigma^+_{0^+}$ and $b^3\Pi_{0^+}-X^1\Sigma^+_{0^+}$ transitions are observed, and these are found to be analogous to the strongest spin-forbidden system in CO, the Cameron band $a^3\Pi-X^1\Sigma^+$. The experimentally derived T_{00} values of $b^3\Pi_{0+}$ and $b^3\Pi_1$ components are 24 200 and 24 760 cm^{-1}, respectively, which are higher than the MRDCI estimated values by 700−1000 cm^{-1}. The computed ω_e values agree well with the experimental values of Deutsche and Barrow.[10] At r_e, $b^3\Pi_{0^+}$ and $b^3\Pi_{0^-}$ components are relatively pure $b^3\Pi$, while strong coupling with other nearby states is noted for the remaining two components of $b^3\Pi$. Transition probabilities of b $^3\Pi_{0^+}-X$ and $b^3\Pi_1-X$ transitions are important in the present context. As mentioned earlier, the $A^1\Pi_1-X\ ^1\Sigma^+_{0^+}$ band system of SnO has been studied by several authors, and the transition around 28 500 cm^{-1} is expected to be strong. As seen in Table 3, the $^3\Pi_1$ component interacts with $A^1\Pi_1$ weakly. The $E^1\Sigma^+_{0^+}$ component does not couple with any nearby state significantly. However, the E−X transition around 34 250 cm^{-1} is expected to be strong.

V. Transition Properties

Two bound singlet states of SnO, namely, $E^1\Sigma^+$ and $A^1\Pi$, are chosen for the symmetry allowed transitions to the ground state in the absence of any spin−orbit coupling. Transition probabilities of these two transitions: $E^1\Sigma^+-X$ and $A^1\Pi-X$ have been computed from the MRDCI wave functions and energies. Both the transitions are reasonably strong. In Figure 3a, we have shown transition dipole moment curves of three transitions computed here. The transition-moment curve of E−X shows a maximum in the Franck−Condon region, while the curve of A−X is monotonically decreasing with bond length. In general, the computed transition moments of E−X are found to be larger than those of the A−X transition in the bond length region above $r = 3.5\ a_0$. Moreover, the $E^1\Sigma^+$ state lies well above $A^1\Pi$, which makes the E−X transition more probable than A−X. Dube and Rai[15] have calculated oscillator strengths ($f_{v'v''}$) for the $A^1\Pi-X^1\Sigma^+$ system of SnO from the measurement of band intensities using the photographic photometry method. The $f_{v'v''}$ values computed here for the same $A^1\Pi-X^1\Sigma^+$ band are found to be larger than the experimentally derived values by a factor of 10. The MRDCI estimated radiative lifetimes of E and A at the lowest vibrational level are about 50 and 140 ns, respectively (Table 4). These values do not change much at the higher vibrational levels. Two triplet−triplet transitions, namely $b^3\Pi-a^3\Sigma^+$ and $b^3\Pi-{}^3\Delta$ are possible to take place. The transition dipole moment values of both the transitions are quite small, which in addition to the smaller energy differences make these transitions less probable. It may be noted that the potential energy curves of $^3\Delta$ and $b^3\Pi$ cross near the equilibrium bond length of the b state (see Figure 1). Because of the different r_e values of these two states, the Franck−Condon factor is too small for computing the transition probability of the $b^3\Pi-a^3\Delta$ transition. The transition-moment curve of $b^3\Pi-a^3\Sigma^+$ is smooth and crosses zero around 4.8 a_0 (see Figure 3a). The computed partial radiative lifetime of $b^3\Pi$ is 296 μs. In the presence of the spin−orbit coupling, transition probabilities of both $A^1\Pi_1-X^1\Sigma^+_{0^+}$ and $E^1\Sigma^+_{0^+}-X^1\Sigma^+_{0^+}$ do not change significantly. Transition dipole moment curves of these two transitions are shown in Figure 3b. The estimated partial lifetimes of $E^1\Sigma^+_{0^+}$ and $A^1\Pi_1$ at the lowest vibrational level remain unchanged. Other transitions ($\Delta\Omega = 0, \pm1$) from these two components are too weak to have any effect on the intensities of $E^1\Sigma^+_{0^+}-X$ and $A^1\Pi_1-X$ transitions. We have reported transition moments of two important spin-forbidden transitions, namely $b^3\Pi_1-X$ and $b^3\Pi_{0^+}-X$ which are experimentally observed. The partial lifetimes of $b^3\Pi_1$ and $b^3\Pi_{0^+}$ are calculated to be 4.3 and 58.1 μs, respectively, at $v' = 0$. Hence the $b^3\Pi_1-X$ transition is found

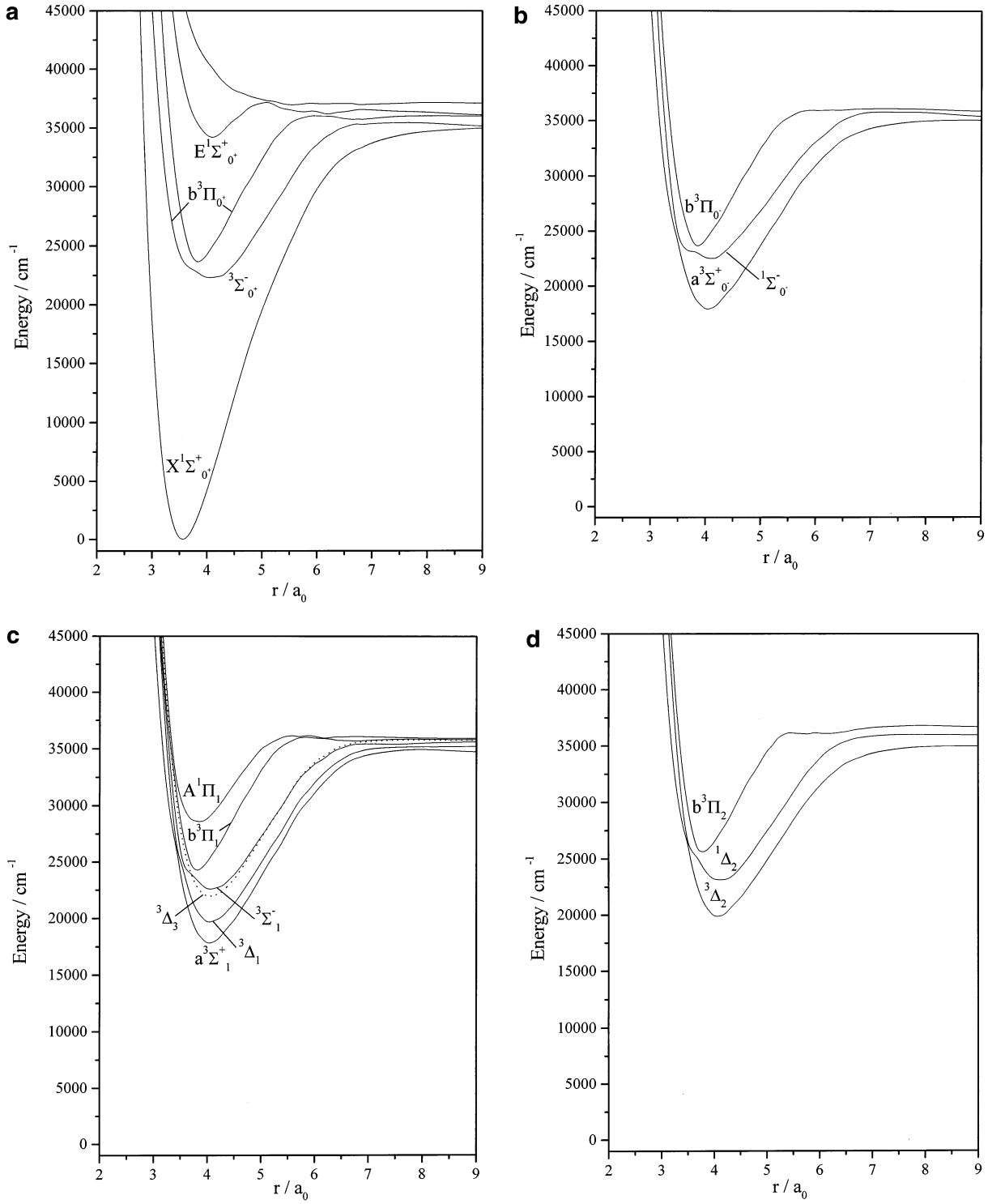

Figure 2. Computed potential energy curves of Ω states of SnO for (a) $\Omega = 0^+$, (b) $\Omega = 0^-$, (c) $\Omega = 1$ and 3, and (d) $\Omega = 2$.

to be stronger than the other. This is because of the stronger mixing of the $A^1\Pi_1$ component in $b^3\Pi_1$. The d-electron correlation does not influence the transition properties and lifetimes significantly.

The dipole moment curves of the SnO molecule in three electronic states, namely, $X^1\Sigma^+$, $A^1\Pi$, and $E^1\Sigma^+$ as a function of the internuclear distance are shown in Figure 3c. All three curves have identical patterns. The largest absolute values of the dipole moment of these states are obtained between 4.5 and 5.0 a_0. It may be mentioned that all curves in Figure 3a−c would tend to zero at large r as all atomic transitions are dipole-forbidden and the atoms are neutral. We have verified that the transition and dipole moment values are nearly zero above $r =$ 20 a_0. Figure 3a−c have shown only the Franck−Condon region. For the ground state, the dipole moment of SnO maximizes ($D = -1.74\ ea_0$) at 4.8 a_0. The negative sign corresponds to the Sn^+-O^- polarity. At the equilibrium bond length, the ground-state dipole moment of SnO estimated in the present calculation without d-correlation is $-1.41\ ea_0$, which is found to be smaller than the experimental value of $-1.70 \pm 0.04\ ea_0$[49,51] obtained from the Stark-effect measurements of pure rotational transitions of the $^{120}Sn^{16}O$ molecule. Kellö and

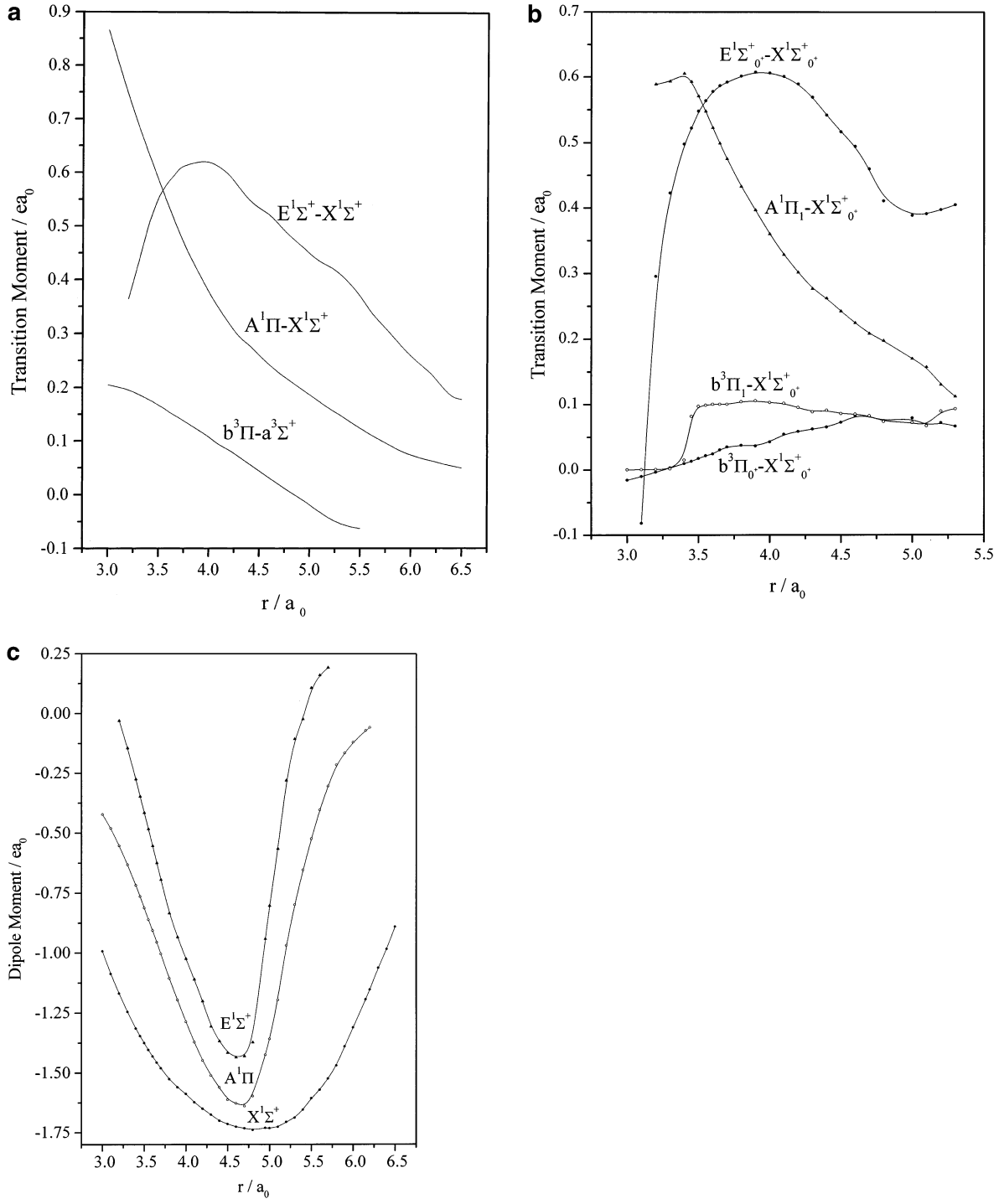

Figure 3. (a) Transition-moment curves of three transitions involving Λ−S states of SnO. (b) Transition-moment curves of four transitions involving Ω states of SnO. (c) Dipole-moment functions of $X^1\Sigma^+$, $A^1\Pi$, and $E^1\Sigma^+$ states of SnO.

Sadlej[25] have reported a dipole moment of −1.44 ea_0 from the numerical finite field perturbation calculations. On the other hand, the coupled cluster method with single and double excitations and perturbative correction from the triple excitations have estimated $\mu = -1.59\ ea_0$ for the ground-state SnO molecule. The present calculations reveal that the d-correlation does not have any significant effect on the ground-state dipole moment of the molecule. The computed dipole moments of the $A^1\Pi$ and $E^1\Sigma^+$ states are −1.21 and −1.09 ea_0 at their respective equilibrium bond lengths. Both $\sigma \rightarrow \pi^*$ and $\pi \rightarrow \pi^*$ transitions in these two excited states tend to move the electronic charge in the direction of Sn, thereby lowering the dipole moment from the ground-state value.

TABLE 4: Computed Radiative Lifetimes (μs) of Some Excited States for the Lowest Three Vibrational Levels

	partial lifetime of the upper state		
transition	$v' = 0$	$v' = 1$	$v' = 2$
$E^1\Sigma^+ - X^1\Sigma^+$	0.05	0.06	0.06
$A^1\Pi - X^1\Sigma^+$	0.14	0.14	0.14
$b^3\Pi - a^3\Sigma^+$	296	257	234
$E^1\Sigma^+_{0+} - X^1\Sigma^+_{0+}$	0.05	0.06	0.06
$A^1\Pi_1 - X^1\Sigma^+_{0+}$	0.14	0.14	0.14
$b\ ^3\Pi_{0+} - X^1\Sigma^+_{0+}$	58.1	68.7	54.5
$b^3\Pi_1 - X^1\Sigma^+_{0+}$	4.3	4.1	4.5

VI. Summary of the Results

A large number of low-lying electronic states of SnO has been computed by using RECP based MRDCI method. The ground state ($X^1\Sigma^+$) of the SnO molecule is represented mainly by a closed shell configuration $\sigma^2\pi^4$. The calculated r_e of the ground state is overestimated by about 0.05 Å, while the computed ω_e value is smaller than the observed value by 58 cm^{-1}. However, the inclusion of d^{10} electrons of Sn in CI improves the ground-state r_e and ω_e by 0.02 Å and 53 cm^{-1}, respectively. Among the other low-lying excited states, a $^3\Sigma^+$, $b^3\Pi$, $A^1\Pi$, $E^1\Sigma^+$, and their spin−orbit components, are important from the experimental point of view. Transition energies of these states are always found to be somewhat lower than the available experimental values. The d-correlation is found to improve the spectroscopic parameters of Σ and Δ states more than those of Π states. There is a strong configuration mixing in the $E^1\Sigma^+$ state, while other bound states are relatively pure. At the lower level of accuracy, the existence of $3^1\Pi$ has been noted around 53 600 cm^{-1}. Transitions from $A^1\Pi$ and $E^1\Sigma^+$ to the ground state are found to be highly probable. The present calculations suggest that $E^1\Sigma^+-X^1\Sigma^+$ is the strongest transition of all. The estimated radiative lifetimes of $E^1\Sigma^+$ and $A^1\Pi$ are 50 and 140 ns, respectively. The inclusion of the spin−orbit coupling introduces several avoided curve crossings in the potential energy curves of Ω-states. In the Franck−Condon region, some mixings have been noted. The present calculations indicate that the spin-forbidden transition such as a $^3\Sigma_1^+-X^1\Sigma_{0^+}^+$ should take place around 17 900 cm^{-1}, which is somewhat smaller than the observed value. The estimated radiative lifetime of a $^3\Sigma_1^+$ at the lowest vibrational level is in the millisecond order. Both b $^3\Pi_{0^+}-X^1\Sigma_{0^+}^+$ and $b^3\Pi_1-X^1\Sigma_{0^+}^+$ transitions, which are analogous to the Cameron band of isovalent CO, have been found to be more probable than a−X. The former transition is expected to be 10 times weaker than the latter.

Acknowledgment. K.K.D. thanks CSIR, Government of India, for the financial support under the Scheme 01 (1759)/02/EMR-II. D.G. also thanks CSIR for the award of a Junior Research Fellowship.

References and Notes

(1) Sutton, D. G.; Suchard, S. N. *Appl. Opt.* **1975**, *14*, 1898.
(2) Felder, W.; Fontijn, A. *Chem. Phys. Lett.* **1975**, *34*, 398.
(3) Mahanti, P. C. *Z. Phys.* **1931**, *68*, 114.
(4) Jevons, W. *Proc. Phys. Soc.* **1938**, *50*, 910.
(5) Lagerqvist, A.; Lennart-Nilsson, N. E.; Wigartz, K. *Ark. Fys.* **1959**, *15*, 521.
(6) Loomis, F. W.; Watson, T. F. *Phys. Rev.* **1934**, *45*, 805.
(7) Sen Gupta, A. K. *Proc. Phys. Soc.* **1939**, *51*, 62.
(8) Eisler, B.; Barrow, R. F. *Proc. Phys. Soc.* **1949**, *62*, 740.
(9) Barrow, R. F.; Rowlinson, H. C. *Proc. R. Soc.* **1954**, *A224*, 374.
(10) Deutsch, E. W.; Barrow, R. F. *Nature* **1964**, *201*, 815.
(11) Nair, K. P. R.; Singh, R. B.; Rai, D. K. *J. Chem. Phys.* **1965**, *43*, 3570.
(12) Smith, J. J.; Meyer, B. *J. Mol. Spectrosc.* **1968**, *27*, 304.
(13) Meyer, B.; Smith, J. J.; Spitzer, K. *J. Chem. Phys.* **1970**, *53*, 3616.
(14) Joshi, M. M.; Yamdagni, R. *Ind. J. Phys.* **1967**, *41*, 275.
(15) Dube, P. S.; Rai, D. K. *J. Phys. B: At. Mol. Phys.* **1971**, *4*, 579.
(16) Capelle, G. A.; Linton, C. *J. Chem. Phys.* **1976**, *65*, 5361.
(17) Marino, C. P.; Guerin, J. D.; Nixon, E. R. *J. Mol. Spectrosc.* **1974**, *51*, 160.
(18) Balasubramanian, K.; Pitzer, K. S. *Chem. Phys. Lett.* **1983**, *100*, 273.
(19) Balasubramanian, K. *J. Phys. Chem.* **1984**, *88*, 5759.
(20) Dyke, J. M.; Morris, A.; Ridha, A. M. A.; Snijders, J. G. *Chem. Phys.* **1982**, *67*, 245.
(21) Balasubramanian, K. *Chem. Rev.* **1989**, *89*, 1801.
(22) Balasubramanian, K. *Relativistic Effects in Chemistry Part A. Theory and Techniques*; Wiley-Interscience: New York, 1997.
(23) Balasubramanian, K. *Relativistic Effects in Chemistry Part B. Applications to Molecules and Clusters*; Wiley-Interscience: New York, 1997.
(24) Kellö, V.; Sadlej, A. J.; Faegri, Jr., K. *J. Chem. Phys.* **1998**, *108*, 2056.
(25) Kellö, V.; Sadlej, A. J. *J. Chem. Phys.* **1993**, *98*, 1345.
(26) Lefebvre, I.; Szymanski, M. A.; Olivier-Fourcade, J.; Jumas, J. C. *Phys. Rev. B* **1998**, *58*, 1896.
(27) Chattopadhyaya, S.; Chattopadhyay, A.; Das, K. K. *J. Phys. Chem.* **2002**, *A106*, 833.
(28) Dutta, A.; Chattopadhyaya, S.; Das K. K. *J. Phys. Chem.* **2001**, *A105*, 3232.
(29) Manna, B.; Das, K. K. *J. Phys. Chem.* **1998**, *A102*, 214.
(30) Dutta, A.; Manna, B.; Das, K. K. *Ind. J. Chem.* **2000**, *39A*, 163.
(31) Krauss, M.; Stevens, W. J. *Annu. Rev. Phys. Chem.* **1984**, *35*, 357.
(32) Christiansen, P. A.; Ermler, W. C.; Pitzer, K. S. *Annu. Rev. Phys. Chem.* **1985**, *36*, 407.
(33) Balasubramanian, K.; Pitzer, K. S. *Adv. Chem. Phys. Chem.* **1987**, *67*, 287.
(34) Gropen, O. In *Methods in Computational Chemistry*; Wilson, S., Ed.; Plenum: New York, 1988; p 109.
(35) LaJohn, L. A.; Christiansen, P. A.; Ross, R. B.; Atashroo, T.; Ermler, W. C. *J. Chem. Phys.* **1987**, *87*, 2812.
(36) Pacios, L. F.; Christiansen, P. A. *J. Chem. Phys.* **1985**, *82*, 2664.
(37) Alekseyev, A. B.; Liebermann, H.-P.; Buenker, R. J.; Hirsch, G. *Mol. Phys.* **1996**, *88*, 591.
(38) Alekseyev, A. B.; Liebermann, H.-P.; Buenker, R. J.; Hirsch, G.; Li, Y. *J. Chem. Phys.* **1994**, *100*, 8956.
(39) Balasubramanian, K. *Chem. Phys. Lett.* **1987**, *139*, 262.
(40) Buenker, R. J.; Peyerimhoff, S. D. *Theor. Chim. Acta* **1974**, *35*, 33.
(41) Buenker, R. J.; Peyerimhoff, S. D. *Theor. Chim. Acta* **1975**, *39*, 217.
(42) Buenker, R. J.; Peyerimhoff, S. D.; Butscher, W. *Mol. Phys.* **1978**, *35*, 771.
(43) Buenker, R. J. *Int. J. Quantum Chem.* **1986**, *29*, 435.
(44) Buenker, R. J. In *Proceedings of the Workshop on Quantum Chemistry and Molecular Physics*; Burton, P., Ed.; University Wollongong: Wollongong, Australia, 1980.
(45) Buenker, R. J. In *Studies in Physical and Theoretical Chemistry*; Carbó, R., Ed.; Elsevier: Amsterdam, The Netherlands, 1981; Vol. 21 (Current Aspects of Quantum Chemistry).
(46) Buenker, R. J.; Phillips, R. A. *J. Mol. Struct. (THEOCHEM)* **1985**, *123*, 291.
(47) Davidson, E. R. In *The World of Quantum Chemistry*; Daudel, R., Pullman, B., Eds.; Reidel: Dordrecht, The Netherlands, 1974.
(48) Hirsch, G.; Bruna, P. J.; Peyerimhoff, S. D.; Buenker, R. J. *Chem. Phys. Lett.* **1977**, *52*, 442.
(49) Huber, K. P.; Herzberg, G. In *Molecular Spectra and Molecular Structure*; Van Nostrand Reinhold: Princeton, NJ, 1979; Vol. 4 (Constants of Diatomic Molecules).
(50) Colin, R.; Drowart, J.; Verhaegen, G. *Trans. Faraday Soc.* **1965**, *61*, 1364.
(51) Hoeft, J.; Lovas, F. J.; Tiemann, E.; Tischer, R.; Törring, T. *Z. Naturforsch.* **1969**, *24a*, 1222.
(52) Moore, C. E. *Tables of Atomic Energy Levels*; U.S. National Bureau of Standards: Washington, DC, 1971; Vols. I−III.